IEEE Access
Multidisciplinary | Rapid Review | Open Access Journal

Received 3 April 2023, accepted 16 May 2023, date of publication 24 May 2023, date of current version 14 June 2023.

Digital Object Identifier 10.1109/ACCESS.2023.3279735

APPLIED RESEARCH

Handwritten Digits Recognition From sEMG: Electrodes Location and Feature Selection

ANDREA TIGRINI, (Member, IEEE), FEDERICA VERDINI, (Member, IEEE), MARA SCATTOLINI, (Graduate Student Member, IEEE), FEDERICO BARBAROSSA, LAURA BURATTINI, (Member, IEEE), MICAELA MORETTINI, (Member, IEEE), SANDRO FIORETTI, (Member, IEEE), AND ALESSANDRO MENGARELLI, (Member, IEEE)
Department of Information Engineering, Università Politecnica delle Marche, 60131 Ancona, Italy

Corresponding author: Alessandro Mengarelli (a.mengarelli@staff.univpm.it)

This work involved human subjects or animals in its research. Approval of all ethical and experimental procedures and protocols was granted by the Institutional Ethics Committee of the Università Politecnica delle Marche, and in line with the Declaration of Helsinki.

ABSTRACT Despite hand gesture recognition is a widely investigated field, the design of myoelectric architectures for detecting finer motor task, like the handwriting, is less studied. However, writing tasks involving cognitive loads represent an important aspect toward the generalization of myoelectric-based human-machine interfaces (HMI), and also for many rehabilitative tasks. In this study, the handwriting recognition of the ten digits was faced under the myoelectric control perspective, considering the probes setup and the feature extraction step. Time and frequency domain features were extracted from surface electromyography (sEMG) signals of 11 subjects who wrote the ten digits following a standardized template and 8 sEMG probes were equally distributed between forearm and wrist. Feature class separability was investigated and an aggregated feature set was built to train pattern recognition architectures, i.e. linear discriminant analysis (LDA) and quadratic support vector machine (QSVM). Also, four reduced probes setups were investigated. LDA and QSVM showed mean accuracy of about 97%, with all the forearm and wrist sEMG information. A significant reduction of performances was observed considering the wrist or the forearm only ($\leq$92%) and when LDA and QSVM were trained with two electrodes information ($\leq$90%). For the reliable classification performances in a motor task involving high cognitive demands, like the handwriting, it is required the use of probes fully covering forearm and wrist. Outcomes support the methodological transfer from myoelectric hand gesture to the handwriting recognition, which represents a key aspect in the development of new HMI for rehabilitation tasks.

INDEX TERMS Handwriting, myoelectric pattern recognition, feature extraction, human-machine interface.

I. INTRODUCTION

Recently, the use of surface electromyography (sEMG) for human-machine interfaces (HMI) is finding a widespread consensus in the literature [1], [2], [3], [4]. Indeed, myoelectric control proved to be valuable in different fields, i.e. from robotics to prosthesis, where the sEMG signals are used for decoding human intent in high-level control architectures [3], [5], [6]. This signal can be used to opportunely interact in virtual and augmented reality scenarios, substantially contributing to the development of sEMG-based HMI [7], [8], [9], [10] for gaming and medical diagnosis aims [2], [11].

Despite, both proportional and pattern recognition architectures (PRA) can be employed for the development of HMI [2], [3], [12], the PRA solutions demonstrated to be particularly appealing and widely employed in real applications [13]. However, it is desirable to select commands from a large set of possible hand gestures since it allows to make more rich and fluent the human-machine interaction [2], [3]. This can be reached by considering finer movements of

The associate editor coordinating the review of this manuscript and approving it for publication was Xianzhi Wang.

the hand in addition to the commonly used set of grasps, fingers, and wrist motions [14], [15], [16]. Such tendency can be recognized in recent studies, where a large number of gestures is taken into account in designing PR architectures for myoelectric control [2], [17]. Moreover, the technological advancements observed in the field of wearable devices shifted the attention to new devices that can be placed either on the forearm or on the wrist [2], [14]. In particular, the information acquired by sensing muscles activity closed to such joint appeared to be promising for developing HMI and the interest to change the focus from forearm to wrist in the development of EMG-based HMI was confirmed in [2]. Indeed, the PRA trained on wrist data provided similar or superior performances with respect to those based on forearm EMG signals [2]. Such change of perspective can be justified not only by the goodness of the results, but also by the needs behind the development of minimally cumbersome interfaces [2].

The assessment of PRA based on wrist EMG data deserves to be further investigated to get a deeper awareness of the potential role that such joint can play for the above mentioned purposes. Thus, to understand whether the wrist can be a reliable landmark, it appears reasonable to investigate more challenging hand movements involving a finer motor control. For this reason, in this work, the recognition of handwritten digits on paper, based on forearm and wrist myoelectric activity, was faced. In the handwriting, the central nervous system integrates visual-spatial information and regulates all the subtle contractions of the upper limb muscles, in order to adjust the movement of the pen [18], [19]. This produces synergistic muscle activation of the hand, wrist, and forearm muscles that may challenge the automatic recognition of complex task as the handwriting.

As a matter of fact, in previous studies [6], [20], [21], [22], the recognition of a hand written characters from sEMG data was faced through template matching, dynamic time warping, and deep learning approaches, which require large databases with a high computational burden in the training step. For instance, in [22] each subject wrote 36 characters on a screen, and each character was repeated one thousand times in order to create the dataset. This unavoidably hampers its application in a practical scenario, since the subject has to undergo long acquisition sessions. Further, similarly to [21], before the classification step, sEMG data were mapped in pen coordinates, acquired upon the plane. This is consistently different with respect to the approaches employed in the classical hand gesture recognition field, where typical data labeling and machine learning techniques are adopted [2], [12], [23], [24].

The aim of this study is to understand whether it is possible to detect the hand-written digits through PRA specific for the EMG based hand gesture recognition [2], [14], [23], extending such methodologies toward a not fully investigated motor task. Moreover, it has been also investigated the role played by the wrist in the development of sEMG-based PRAs for handwritten digits recognition. For these purposes, an opportune dataset was collected taking into account 11 subjects who wrote all the digits by matching a given template. Then, multiple PRA were trained taking into account different electrodes setups, i.e. considering data coming from forearm channels, wrist channels, and considering all the channels together.

(a)

(b)

FIGURE 1. Eight EMG electrodes configuration. Panels 1(a) and 1(b) show how sEMG probes were distributed respectively on the frontal and ventral part of the arm.

II. MATERIALS AND METHODS

A. DATA COLLECTION

Eight self-adhesive bipolar surface electrodes (BTS Bioengineering FREEEMG) with sampling frequency 1000 Hz were used. Four probes were placed around the proximal forearm, whereas the remaining surrounded the wrist circumferentially [2]. In particular, following the electrode placement in [2], two forearm probes were placed over the extensor digitorum (channel 1, CH1) and flexor carpi radialis (channel 2, CH2). The other two electrodes were equidistantly located on the opposite side of the forearm, covering brachioradialis (channel 3, CH3) and flexor carpi ulnaris respectively (channel 4, CH4) (Fig. 1). Regarding the wrist electrodes, two probes covered extensor digitorum minimi (channel 5, CH5) and extensor digiti (channel 6, CH6), on the posterior side of the wrist proximally to the ulnar styloid process. The other two probes were arranged on the anterior side of the wrist, covering distal ending of flexor carpi radialis in correspondence to the deep flexor pollicis longus (channel 7, CH7) and flexor digitorum superficialis (FD, CH8), respectively (Fig. 1).

B. EXPERIMENTAL PROTOCOL

For the experiment, 11 healthy subjects, 6 males and 5 females aged between 21 and 50, were recruited. All

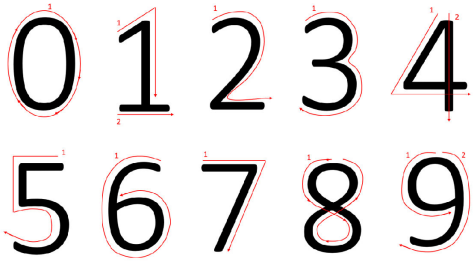

FIGURE 2. Template of ten digits. Red arrows indicate the writing pattern. Note that digit 4 and 9 are multi-stroke signs whereas all other digits are single stroke.

participants gave their written informed consent and the study was approved by the institutional ethic committee. Volunteers were asked to write numbers from 0 to 9 with their dominant hand, sitting in a comfortable position and leaning the arm against desk to avoid fatigue during the task. In order to standardize the writing pattern of every digit, a standard template of numbers is followed, as shown in Fig. 2. Each digit was written ten time and subjects alternated a writing phase of 3 seconds and a resting phase of 5 seconds for every repetition, resulting in a total duration of about 15 minutes for each experiment.

C. SIGNAL PRE-PROCESSING

All the raw sEMG signals underwent the same pre-processing steps. Signal amplitude was normalized with respect to the maximum peak value. A second order, zero phase, band-pass Butterworth filter with 30 Hz lower cut-off frequency and 450 Hz higher cut-off frequency was applied. An ON-OFF time instants detection was performed in order to extract features in the contraction phase [14], [25]. An example of the sEMG signals recorded from a trial were reported in Fig. 3. At the end of this process, data are organized in a 10×8 array (10 activations $\times$ 8 recordings).

Each detected activation burst was then segmented with 150 ms length windows overlapping of 75 ms each other, consistently with common practice in myoelectric pattern recognition problems [26], [27], [28]. Eventually, for each subject, a total of 3900 samples were obtained for training and testing machine learning models.

D. FEATURE EXTRACTION AND ANALYSIS

Selection and extraction of highly effective features is one of the most crucial aspect in pattern recognition and myoelectric control design [12], [29]. To this point, two kind of analysis were performed. As first, a total of 26 features were extracted form each sEMG segment: 16 time-domain (TD) and 10 frequency-domain (FD) features [2], [4], [14]. Each feature dimension depends both on the number of channels and on the type of feature, i.e. single or multi-dimensional. By indicating n as the number of channel considered, the feature dimension is obtained accordingly as reported in Table 1.

Then, they were aggregated in sets made by the same features computed for all the channels. For each of these data sets, a class separability assessment (Section II-E) was performed in order to verify the capabilities of each feature in highlighting the myoelectric patterns.

The second analysis regarded the evaluation of PRA over an aggregated feature set obtained by including the TD and FD features that respectively showed the best separability properties. Hence, such feature set was considered in different sEMG channels configurations:

- all the channels of the forearm and wrist (ALL);
- the forearm channels, i.e. from 1 to 4 (FA);
- the forearm reduced setup 1, i.e. channels 1 and 2 (FA1);
- the forearm reduced setup 2, i.e. channels 3 and 4 (FA2);
- the wrist channels, i.e. from 5 to 8 (WR);
- the wrist reduced setup 1, i.e. channels 5 and 6 (WR1);
- the wrist reduced setup 2, i.e. channels 7 and 8 (WR2).

Please, notice that, in accordance with Table 1, feature space dimension is 48 for ALL, 24 and 12 for FA, WR and FA1, FA2, WR1, WR2, respectively. This was done in order to asses how different setup configurations impact on the performances of PRA. Please note that all the reduced setups, i.e. FA1, FA2, WR1 and WR2 encompasses a couple of agonist/antagonist muscles. This guaranteed a functional and minimal covering for the hand tasks.

E. CLASS SEPARABILITY PROPERTIES

In the first analysis, three indexes were computed to evaluate the cluster separability properties of each EMG feature space. The first two indexes were the separability index (SI) and the mean semi-principal axis (MSA) [30], [31]. The former quantifies the distances between the different clusters present in a data set, hence mirroring how much the classes are separable. The SI can be computed as [30] and [32]:

$$SI = \frac{1}{N}\sum_{j=1}^{N}\left(\frac{1}{2}\sqrt{(\mu_j - \mu c_j)^T S^{-1}(\mu_j - \mu c_j)}\right) \tag{1}$$

where N is the number of classes, μ_j is the centroid of class j, μ_{Cj} is the centroid of the most conflicting class (with respect to class j), and S is defined as:

$$S = \frac{S_j + S_{Cj}}{2} \tag{2}$$

where S_j is the covariance of class j and S_{Cj} is the covariance of the most conflicting class (with respect to class j). The larger the SI value, the more distinct the classes are [30].

The MSA was proposed as a measure for intra-class variability and it considers the points of each class as a cluster in the shape of a hyper-ellipsoid [31], complementing the information provided by the SI. Indeed, it may happen that an increase in classes separability may result from clusters that are compact, or from clusters that are located farther apart. Thus, accessing information on distribution of data within single class and evaluating the spatial size of cluster is an important aspect to take into account.

TABLE 1. Features extracted for time and frequency domains. More information regarding their computation can be found in [12], [14], [24], and [29]. Last column of the table reports the dimension of the feature, which depends on the number n of channels considered.

Type	FeatureName	Abbreviation	Dimension
TD	Integrated EMG	IEMG	n° of channels
	Mean Absolute Value	MAV	n° of channels
	Variance of sEMG	VAR	n° of channels
	Root Mean Square	RMS	n° of channels
	Waveform Length	WL	n° of channels
	Difference Absolute Mean Value	DAMV	n° of channels
	Difference Absolute Standard Deviation Value	DASDV	n° of channels
	Zero Crossing	ZC	n° of channels
	Myopulse Percentage Rate	MYOP	n° of channels
	Willison Amplitude	WAMP	n° of channels
	Slope Sign Change	SSC	n° of channels
	Fuzzy Entropy	FuzEn	n° of channels
	Permutation Entropy	PermEn	n° of channels
	Histogram of EMG, 10-bins	HIST	10× n° of channels
	Auto-Regressive Coefficients, 4^{th} Order	AR	4 × n° of channels
	Cepstrum coefficients of the 4^{th} Order AR process	CC	4 × n° of channels
FD	Mean Frequency	MNF	n° of channels
	Median Frequency	MDF	n° of channels
	Peak Frequency	PKF	n° of channels
	Total Power	TTP	n° of channels
	1^{st} Spectral Moment	SM1	n° of channels
	2^{nd} Spectral Moment	SM2	n° of channels
	3^{rd} Spectral Moment	SM3	n° of channels
	Frequency Ratio	FR	n° of channels
	Power Spectrum Ratio	PSR	n° of channels
	Variance of Central Frequency	VCF	n° of channels

MSA can be computed as:

$$MSA = \frac{1}{N}\sum_{j=1}^{N}((\prod_{k=1}^{n} a_{jk})^{\frac{1}{n}}) \tag{3}$$

where a a_{jk} is the k^{th} of n singular values of class j and n is equal to the number of feature space dimensions. The n value varies according to the number of features contained in each feature set. Thus, the greater is the density of the clusters the lower is the variability among data, resulting in a lower MSA.

A further index commonly employed to asses the class separability properties was the Davies-Bouldin (DB) [2], [33]:

$$DB = \frac{1}{N}\sum_{i=1}^{N} max(R_{ij}) \tag{4}$$

where R_{ij} is cluster similarity

$$R_{ij} = \frac{S_i + S_j}{D_{ij}} \tag{5}$$

S_i and S_j are the dispersions of the i^{th} and j^{th} clusters respectively, and D_{ij} is the distance between their mean value. In other words, the DB index describes how badly the clusters overlap their closest neighbors [34]. Thus, lower values of the DB index stand for a higher degree of cluster separability.

F. CLASSIFICATION EXPERIMENTS

A first comparison was performed using the eight sEMG channels in order to test the goodness of feature selected through class separability metrics with respect to all the features, i.e., TD and FD, and with respect to a feature set obtained by a gold-standard feature selection procedure [2], [28]. In particular, a modified version of the forward feature selection algorithm (FFS) was used to select those features that were more representative of the population, avoiding possible bias effects due to individual characteristics and probes location. For this reason, the FFS selected the features that minimizes the ten-fold validation error averaged among the 11 subjects by adding at each step the same block of feature computed over all the channels. Then, the feature set made by the features that showed the best class separability

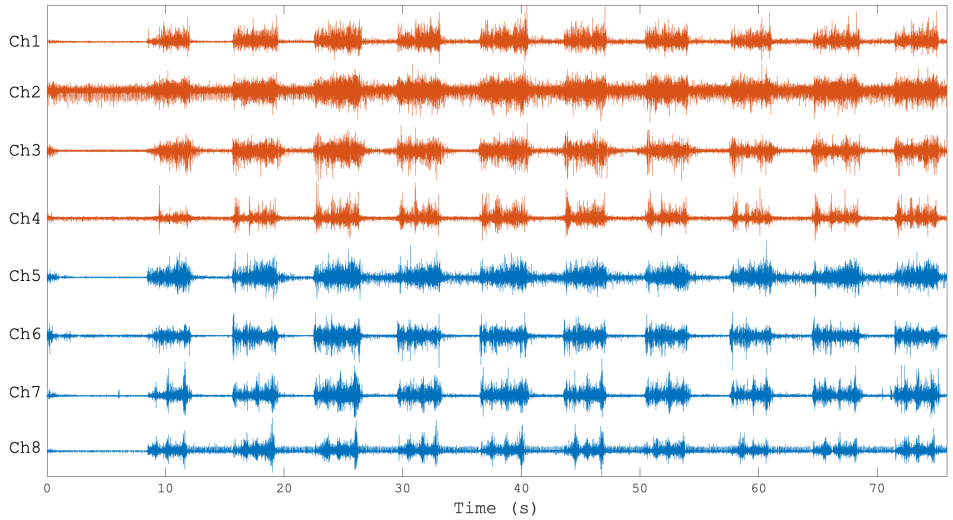

FIGURE 3. The eight sEMG signals obtained from an experimental record of a representative subject. Red traces are relative to the forearm probes, whereas blue traces indicate probes placed on the writs.

properties was employed for PRA experiments in 7 different conditions, as reported in Section II-D.

Two types of PRA that showed reliable performances in myoelectric control were used: the linear discriminant analysis (LDA) classifier, and the support vector machine with a quadratic kernel (QSVM) [2], [23], [35], [36]. These architectures were trained and validated through a ten fold cross validation. In particular, in order to reduce possible issues due to data leakage problems, a class-balanced random split was employed to create the folds. This broke possible time correlation among them, that otherwise can lead to over-optimistic models. The within subject accuracy (WSA), averaged over the ten folds and the macro F1 score were used as metrics to evaluate the performances of both LDA ans QSVM [37].

For each setup condition, pair comparisons between the LDA and QSVM accuracy were performed through the Wilcoxon rank sum test [25]. This was done to assess whether one PRA presented actual advantages with respect to the other one for the considered motor task. Further, the aforementioned statistical test was used for other comparisons involving different setup condition. In particular, WSA obtained in the ALL condition was compared with those provided in FA and WR ones (Section II-D). Following the same line, also the WSA of WR were compared with those in FA. This first set of comparisons was defined in order to understand whether a reduction in the number of recordings of the upper limb muscles activity would degrade the performances of LDA and QSVM. Then, within each anatomical muscles group, i.e. FA and WR, a minimal configuration involving two electrodes would be preferable with respect to the four channels configuration. Hence, WSA provided in FA were compared with those obtained in FA1 and FA2, and the same was done among WR, WR1 and WR2 (second set of comparisons). For each comparison, significance was set at 0.05.

TABLE 2. Mean and standard deviation of MSA, SI and DB value of 11 subjects calculated for time-domain features. The features that presented the best class separability properties are highlighted in bold.

	MSA	SI	DB
MAV	$\mathbf{0.0074 \pm 0.0015}$	$\mathbf{1.08 \pm 0.15}$	$\mathbf{0.72 \pm 0.16}$
VAR	0.0058 ± 0.0017	0.78 ± 0.11	0.58 ± 0.12
RMS	0.0084 ± 0.0014	0.99 ± 0.13	0.73 ± 0.16
WL	0.0068 ± 0.0012	1.15 ± 0.19	0.73 ± 0.15
DAMV	$\mathbf{0.0067 \pm 0.0017}$	$\mathbf{1.15 \pm 0.18}$	$\mathbf{0.73 \pm 0.16}$
DASDV	$\mathbf{0.0075 \pm 0.0014}$	$\mathbf{1.09 \pm 0.16}$	$\mathbf{0.73 \pm 0.15}$
IEMG	0.0074 ± 0.0014	1.06 ± 0.15	0.71 ± 0.17
ZC	0.0143 ± 0.0025	0.32 ± 0.14	0.71 ± 0.06
MYOP	0.0077 ± 0.0056	0.25 ± 0.15	0.65 ± 0.09
WILSON	0.0078 ± 0.0062	0.26 ± 0.16	0.63 ± 0.11
SSC	0.0119 ± 0.0041	0.30 ± 0.15	0.67 ± 0.10
PERMEN	0.0110 ± 0.0046	0.30 ± 0.16	0.66 ± 0.11
FUZZYEN	0.0113 ± 0.0021	0.35 ± 0.13	0.67 ± 0.08
HIST	0.0121 ± 0.0022	0.88 ± 0.21	1.22 ± 0.16
AR	0.0062 ± 0.0017	0.62 ± 0.18	1.36 ± 0.11
CC	0.0068 ± 0.0017	0.63 ± 0.24	1.33 ± 0.12

III. RESULTS

A. CLASS SEPARABILITY PROPERTIES

Table 2 shows the clustering metrics calculated for each time-domain feature, averaged among the 11 subjects. In particular the analysis reported in Section II-E highlighted three TD and three FD features that presented good class separability properties. Concerning the TD ones, MAV, DAMV, DASDV showed the best performances in terms of SI and MSA, whereas the DB showed large set of features with values around 0.7, resulting less sensitive with respect to the other metrics.

The same was done for the FD features (Table 3). The first three spectral moments presented superior separability properties. Indeed, for SM1, SM2, and SM3, the relative lower DB indexes agree with higher SI. Moreover, the MSA values obtained with respect to other FD features indicate that the spectral moments are able to map hand movements in compact clusters. Hence, based on these results, the proposed

TABLE 3. Mean and standard deviation of MSA, SI and DB value of 11 subjects calculated for frequency-domain features. The features that presented the best class separability properties are highlighted in bold.

	MSA	SI	DBI
MNF	0.0120 ± 0.0030	0.39 ± 0.12	0.68 ± 0.15
MDF	0.0155 ± 0.0031	0.34 ± 0.18	0.75 ± 0.19
PKF	0.0044 ± 0.0016	0.56 ± 0.21	0.43 ± 0.08
TTP	0.0058 ± 0.0017	0.78 ± 0.14	0.57 ± 0.19
SM1	$\mathbf{0.0056 \pm 0.0016}$	$\mathbf{0.83 \pm 0.16}$	$\mathbf{0.59 \pm 0.15}$
SM2	$\mathbf{0.0051 \pm 0.0013}$	$\mathbf{0.89 \pm 0.19}$	$\mathbf{0.58 \pm 0.11}$
SM3	$\mathbf{0.0047 \pm 0.0012}$	$\mathbf{0.92 \pm 0.22}$	$\mathbf{0.56 \pm 0.16}$
FR	0.0087 ± 0.0035	0.23 ± 0.21	0.58 ± 0.09
PSR	0.0069 ± 0.0044	0.34 ± 0.14	0.51 ± 0.08
VCF	0.0092 ± 0.0017	0.41 ± 0.29	0.64 ± 0.05

TABLE 4. Table shows the mean WSA of the 11 subjects obtained for LDA and QSVM using ALL condition respectively with the proposed feature set, the one obtained through FFS and all the features together.

PRA	Proposed	FFS	All Features
LDA	97.17±1.89	98.31±0.96	98.02±0.93
QSVM	97.24±1.92	98.37±0.89	99.00±0.95

feature set used in the pattern recognition experiments was composed by MAV, DAMV, DASDV, SM1, SM2 and SM3.

B. PATTERN RECOGNITION EXPERIMENTS

Table 4 shows the mean WSA obtained among the 11 subjects for the proposed feature set, for FFS set and when all the features are used together in ALL condition.The FFS highlighted 8 features, i.e., RMS, WFL,DASDV, SSC, FUZZYEN, SM1, HIST and AR, eventually resulting in a feature space of dimension 160. Such input size is lower if compared to use all the features together, i.e., 360, but consistently higher with respect to the proposed set that has a dimension of 48. Moreover, the proposed feature set has a reduced dimension with respect to the other two feature sets,guaranteeing at the same time no statistically significant drop of accuracy when compared with the other two sets using both LDA and QSVM.

Table 5 shows the mean WSA for the LDA and QSVM architectures in all the setup configurations. For each condition, no statistical difference was observed between the mean WSA provided by LDA and QSVM. This was further supported by the low value of standard deviation obtain in each PRA experiment, i.e. not greater than 2.72%. Regarding the first set of comparisons (Section II-F), the ALL setup configuration performed better than FA and WR, whereas FA showed significant differences with respect to WR. In the ALL case, mean WSA was greater than 97% for both LDA and QSVM, but it reduced in FA and WR, although in the latter case showed values slightly lower than 92% (Table 5).

Regarding the second set of comparisons (Section II-F), FA showed significant greater accuracy with respect to the two reduced configurations FA1 and FA2 (Table 5). However, no significant differences were observed between FA1 and FA2, neither for LDA nor for QSVM. Similarly, WR performed significantly better than WR1 and WR2, whereas no significant difference was observed between the reduced wrist configurations WR1 and WR2. Despite the accuracy were consistently reduced with respect to FA and WR, all the minimal-setup configurations FA1, FA2, WR1, and WR2 showed mean WSA accuracy greater than 86%, indicating good performances even when only two electrodes were used.

Since the gap in the accuracy between FA (WR) and FA1 (WR1), FA2 (WR2) is small, one may wonder whether two channels configuration can be an efficient compromise for practical applications. For this reasons macro F1 was used to further investigate such aspect (see section II-F). Figure 4 reports the mean macro F1 computed for both LDA and QSVM in the reduced sEMG channels conditions. A reduction in the aforementioned metric was observed comparing FA with FA1 and FA2 (Fig. 4(a)) and the same holds also for the WR. Moreover, as shown in Fig. 4, the FA setup provided superior performances if compared with WR, whereas all the reduced configurations did not guaranteed acceptable performances (macro F1 $\leq 70\%$).

IV. DISCUSSION

A. CLASS SEPARABILITY PROPERTIES

The first analyzed aspect regarded the class separability properties of TD and FD features. This step plays a fundamental role when aggregated feature sets are constructed [33]. In the TD, three features appeared to be particularly able in highlighting differences among the ten classes (Table 2). Moreover, as observed in [24], DAMV is calculated exactly as WL, but averaging the latter by the number of window samples, and the same consideration can be pointed out for DASDV and RMS. Hence, although WL and RMS showed good separability properties, the use DAMV and WL (or DASDV and RMS) together in the same feature set is not recommended, since it would increase redundancy without supplying additional information. On the contrary, using either DAMV and DASDV within an aggregated feature set could be a valuable choice since their combined effect provides energy (DASDV) and complexity (DAMV) information contemporaneously [23], [24]. Hence, in this work, based on the above considerations and taking into account the indexes reported in Table 2, the three features selected in TD for defining the aggregated feature set were MAV, DAMV and DASDV. In passing, the inclusion of MAV within the aggregated feature set (Table 2) is not completely surprising since it showed reliable performances in several published studies [12], [14], [38], also when considered alone [24].

Moreover, it deserves to be discussed how the multidimensional features such as HIST, AR and CC behave. The former presents clusters with low aggregation properties, as indicated by the relatively high MSA and DB. This is in agreement with what reported in [23], although some studies highlighted that HIST is a robust feature with respect to electrodes location stability, providing good results when used for myoelectric PRA [30], [33]. A similar behavior holds also for CC and AR, since the inclusion of these two features in an aggregated

TABLE 5. Table shows WSA averaged among the 11 subjects for the seven sEMG channels configurations and for both LDA and QSVM, and for the proposed feature set. Symbols † and ⋆ indicates a significant difference ($p<0.05$) respectively for LDA and QSVM in relation to the first set of comparisons (section II-F). Similarly, symbols ‡ and ∗ indicates a significant difference ($p<0.05$) respectively for LDA and QSVM for the second set of comparisons.

PRA	ALL	FA	FA1	FA2	WR	WR1	WR2
LDA	$97.17\pm1.89^{\dagger}$	$94.28\pm2.41^{\dagger\ddagger}$	$89.14\pm1.34^{\ddagger}$	$88.76\pm3.51^{\ddagger}$	$91.28\pm2.33^{\dagger\ddagger}$	$87.41\pm2.11^{\ddagger}$	$86.84\pm2.34^{\ddagger}$
QSVM	$97.24\pm1.92^{\star}$	$94.86\pm2.27^{\star *}$	$90.05\pm1.22^{*}$	$89.87\pm3.27^{*}$	$92.60\pm2.37^{\star *}$	$88.68\pm2.24^{*}$	$87.37\pm2.72^{*}$

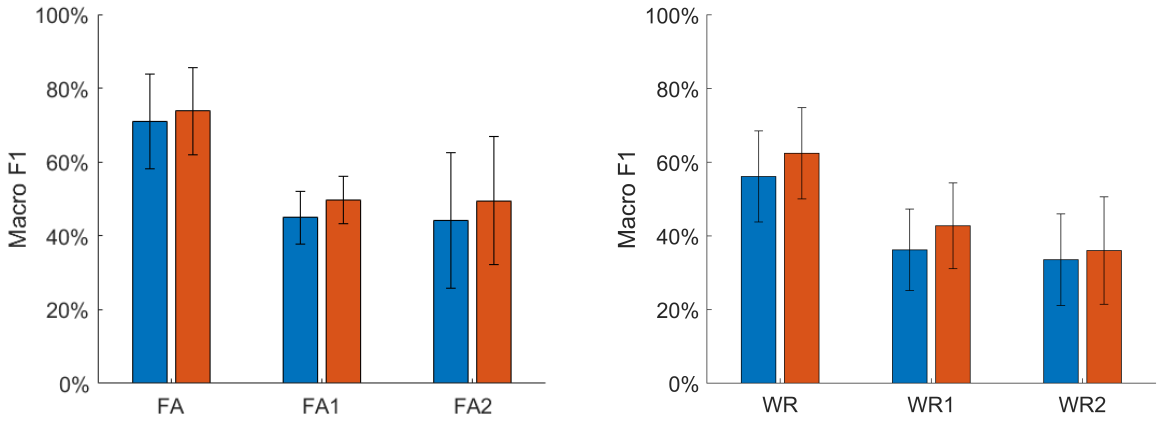

FIGURE 4. Mean *Macro F1* for LDA and QSVM are reported respectively with blue and red bars. Panel 4(a) shows the scores obtained for FA and its relative minimal configurations, i.e. FA1 and FA2. Panel (b) shows the scores obtained for WR and its relative minimal configurations, i.e. WR1 and WR2.

feature set adds meaningful information, generally increasing the overall recognition accuracy [23], [24]. Nevertheless, being CC and AR multidimensional features, they tend to increase the dimensionality of feature space, eventually enhancing the complexity of the PRA and the computational burden in real-time applications.

As observed in Table 3, among the 10 FD features, the first three spectral moments showed the best class separability properties. This confirms that such features have a good capability of mapping EMG signal epochs in well defined patterns [23], [39]. Hence, despite less investigated and used in aggregated datasets, such features were included in the aggregated feature set employed in the present study. Regarding the other FD features, although MNF and MDF were commonly employed in upper limb myoelectric control [40], they showed low class separability properties. This can be due to the small window size adopted for their estimation, since it was reported that the variance of both MNF and MDF grows with a reduction of length of the epoch used for the estimation [41]. This is confirmed by the high MSA values, which indicate relatively less compact clusters, thus characterized by a larger variance.

B. PATTERN RECOGNITION EXPERIMENTS

1) AGGREGATED FEATURE SET AND PRAs

The problem of handwriting recognition through sEMG data is not completely new. Previous studies faced such problem making use of convolutional neural networks or template matching approaches, showing good classification performances [20], [22]. However, such architectures require large data frames to be opportunely trained and validated and this can be a limit in a practical context. Indeed, subjects affected by pathologies cannot undergo to prolonged data acquisition sessions, and this implies the availability of small data sets for the design of PRA [4]. Hence, in this study the problem of handwriting recognition from sEMG data was pursued through LDA and QSVM, which are particularly suitable for the development of myoelectric HMI [2], [30], [36], not requiring large data frames.

The first aim of the PRA experiments in this study regarded the possibility to extend the sEMG-based hand gesture recognition methodologies toward a set of hand movements with a high cognitive demand, such as the handwriting. Results (Section III-B) confirmed that hand written digits recognition can be efficiently performed through myoelectric PRA. In fact, in the ALL channels configuration, mean WSA reached vales of 97.17% and 97.24% for LDA and QSVM respectively, given the proposed feature space. The WSA increases, but not significantly, when FFS set or all the features were used together (Table 4). However, it should be noticed that the input dimension consistently increases in the last two cases since FFS selected a feature space of dimension 160, whereas, combining all the feature together, feature space gets a dimension of 360. This confirms the goodness

of the selection criterion employed, since it allowed to reduce the complexity of the PRA by using those features that showed a priori good clustering properties [33]. Moreover, for the same setup condition no significant differences were observed between the WSA provided by LDA and QSVM, supporting the use of such models for myoelectric PRA applications [30], [36].

To further support the goodness of the proposed set, two state-of-the-art feature set, i.e. Phinyomark 2 and Duan sets [24], [42] were compared to the aggregated one in the ALL condition. Duan set showed mean WSA of 93.88% and 94.96% for LDA and QSVM respectively, which were significantly lower ($p<0.05$) than those reported for the proposed feature set employed in this study. The Phyniomark 2 set showed greater mean WSA with respect to those reported in Table 5, i.e. 97.70% and 97.87% for LDA and QSVM respectively. However, no significant difference has been found between Phinyomark 2 and the aggregated feature set here employed. This indicates that even if Phinyomark 2 employed 7 features per channel, i.e. 4 CC coefficients, PermEn, RMS and WL, it did not significantly boosted the performances of the two PRA if compared to the 6 feature per channel used in the ALL case. Hence, no significant advantages were obtained making use of more complex feature extraction methods, involving nonlinear descriptors or wavelet decomposition [24], [42]. Furthermore, it should be noticed that using FFS [2], [28], or approaching the problem through the clustering metrics [33], have guaranteed a selection of features that were less biased by individual characteristics, and more general for the population. Thus, even if this represents a secondary aspect of the study, it should be noticed that the selected features could be applied to new users, potentially avoiding the search repetition for each new subject.

2) EFFECTS OF REDUCING sEMG CHANNELS IN PR

A further contribution of this study regards the assessment of the sEMG setup in terms of electrodes reduction. This aspect is of great interest in the literature [2], indeed the number of electrodes and their location need to be deeply evaluated in order to realize unobtrusive HMI. In [2], the role of the wrist with respect to the forearm was taken into account by considering up to 16 hand gestures, and the PRA employed showed comparable or superior performances when using wrist sEMG data [2]. However, for a more complex set of motor tasks, like the hand writing, this study shows that the same cannot be stated: as observed in Section 5, FA and WL showed significantly lower performances with respect to the ALL case, whereas FA performed better than WR for both PRA. This indicated that for complex hand motor tasks, an adequate spatial covering is required if one would obtain robust classifiers. Thus, the change of sEMG recording position from forearm to wrist should be evaluated depending on the type of the movements to be recognized. This is confirmed also by the results observed for FA1, FA2, WR1, and WR2. In fact, although the mean WSA slightly lowered passing from FA to FA1 and FA2 and from WR to WR1 and WR2, such drop resulted to be statistically significant (Table 5).

The PRA performance reduction is better highlighted through the macro F1 metric, reported in Fig. 4, where FA1 and FA2 showed consistent lower values with respect to the FA condition (Fig. 4(a)). The same holds for WR if compared to WR1 and WR2 (Fig. 4(b)). As a matter of fact, FA and WR obtained F1 scores greater than 70%, indicating low bias effects in inter-class misclassification [37]. On the other hand, the two-channels configuration showed low F1 values. For instance, the WR2 case presents mean F1 that does not overcome 40% for both LDA and QSVM, suggesting that the trained PRA were able to recognize quite well the given sample, but if the latter is misclassified, it is confused within a subset of other classes, i.e. high accuracy with low F1.

Therefore, the reduction in the PRA performances can be associated to a non optimal muscles covering, mirroring the impossibility to extract enough information from only two sEMG channels, in order to discriminate between the 10 different handwritten digits. This poses the attention on the sensing technology used for extracting muscle information. In fact, as demonstrated in [17], high-density sEMG setups permit to reach high classification performances by recording few muscles but with a high spatial resolution. On the other hand, with sparse sEMG setups, like the one employed in this study, performances can be boosted only by including the information extracted from different muscles [17]. Moreover, despite the WSA is one of the most common metric used for evaluating PRA myoelectric control, relying only on this metric could shadow additional important aspects regarding the robustness of the models [2], [4], [24], [42]. Indeed, although the accuracy slightly reduces when the number of electrodes decreases, the use of a metric that take into account inter-class classification properties such as the macro F1 score can help in preventing undesired PR responses in a real scenario, due to the use of a non-robust implementation.

V. CONCLUSION

In this study, EMG-based PRA were developed to solve the handwriting recognition problem of the ten digits, investigating also the role of sparse sEMG set-up on the forearm and wrist. The results support the possibility to transfer methodologies of the EMG-based hand gesture recognition in the field of handwriting recognition, which represents a key aspect in the development of new HMI for rehabilitation tasks. Further, from the study emerges that a motor task that involves high cognitive demands like the handwriting one requires the use of sEMG electrodes placed both on the forearm and wrist, in order to obtain PRA with WSA greater than 95% and macro F1 greater than 80%. This indicates that a large amount of information is needed when one have to decode fine hand movements, hence suggesting the opportunity to shift from sparse to dense sEMG setup paradigms for the recognition of complex hand motor tasks.

REFERENCES

[1] D. Yang and H. Liu, "An EMG-based deep learning approach for multi-DOF wrist movement decoding," *IEEE Trans. Ind. Electron.*, vol. 69, no. 7, pp. 7099–7108, Jul. 2022.

[2] F. S. Botros, A. Phinyomark, and E. J. Scheme, "Electromyography-based gesture recognition: Is it time to change focus from the forearm to the wrist?" *IEEE Trans. Ind. Informat.*, vol. 18, no. 1, pp. 174–184, Jan. 2022.

[3] X. Jiang, K. Xu, X. Liu, C. Dai, D. A. Clifton, E. A. Clancy, M. Akay, and W. Chen, "Cancelable HD-sEMG-based biometrics for cross-application discrepant personal identification," *IEEE J. Biomed. Health Informat.*, vol. 25, no. 4, pp. 1070–1079, Apr. 2021.

[4] A. Tigrini, L. A. Pettinari, F. Verdini, S. Fioretti, and A. Mengarelli, "Shoulder motion intention detection through myoelectric pattern recognition," *IEEE Sensors Lett.*, vol. 5, no. 8, pp. 1–4, Aug. 2021.

[5] M. Simão, N. Mendes, O. Gibaru, and P. Neto, "A review on electromyography decoding and pattern recognition for human-machine interaction," *IEEE Access*, vol. 7, pp. 39564–39582, 2019.

[6] B. Rodríguez-Tapia, I. Soto, D. M. Martínez, and N. C. Arballo, "Myoelectric interfaces and related applications: Current state of EMG signal processing—A systematic review," *IEEE Access*, vol. 8, pp. 7792–7805, 2020.

[7] U. Côté-Allard, G. Gagnon-Turcotte, A. Phinyomark, K. Glette, E. Scheme, F. Laviolette, and B. Gosselin, "A transferable adaptive domain adversarial neural network for virtual reality augmented EMG-based gesture recognition," *IEEE Trans. Neural Syst. Rehabil. Eng.*, vol. 29, pp. 546–555, 2021.

[8] A. Sharmila, "Hybrid control approaches for hands-free high level human–computer interface—A review," *J. Med. Eng. Technol.*, vol. 45, no. 1, pp. 6–13, Jan. 2021.

[9] Y. Kwon, A. Dwivedi, A. J. McDaid, and M. Liarokapis, "Electromyography-based decoding of dexterous, in-hand manipulation of objects: Comparing task execution in real world and virtual reality," *IEEE Access*, vol. 9, pp. 37297–37310, 2021.

[10] T. Sugiarto, C.-L. Hsu, C.-T. Sun, W.-C. Hsu, S.-H. Ye, and K.-T. Lu, "Surface EMG vs. high-density EMG: Tradeoff between performance and usability for head orientation prediction in VR application," *IEEE Access*, vol. 9, pp. 45418–45427, 2021.

[11] M. Recenti, C. Ricciardi, R. Aubonnet, I. Picone, D. Jacob, H. Á. R. Svansson, S. Agnarsdóttir, G. H. Karlsson, V. Baeringsdóttir, H. Petersen, and P. Gargiulo, "Toward predicting motion sickness using virtual reality and a moving platform assessing brain, muscles, and heart signals," *Frontiers Bioeng. Biotechnol.*, vol. 9, p. 132, Apr. 2021.

[12] S. Micera, J. Carpaneto, and S. Raspopovic, "Control of hand prostheses using peripheral information," *IEEE Rev. Biomed. Eng.*, vol. 3, pp. 48–68, 2010.

[13] N. Nasri, S. Orts-Escolano, and M. Cazorla, "An sEMG-controlled 3D game for rehabilitation therapies: Real-time time hand gesture recognition using deep learning techniques," *Sensors*, vol. 20, no. 22, p. 6451, Nov. 2020.

[14] A. Mengarelli, A. Tigrini, S. Fioretti, S. Cardarelli, and F. Verdini, "On the use of fuzzy and permutation entropy in hand gesture characterization from EMG signals: Parameters selection and comparison," *Appl. Sci.*, vol. 10, no. 20, p. 7144, Oct. 2020.

[15] M. Atzori, A. Gijsberts, C. Castellini, B. Caputo, A.-G.-M. Hager, S. Elsig, G. Giatsidis, F. Bassetto, and H. Müller, "Electromyography data for non-invasive naturally-controlled robotic hand prostheses," *Sci. Data*, vol. 1, no. 1, pp. 1–13, Dec. 2014.

[16] S. Pizzolato, L. Tagliapietra, M. Cognolato, M. Reggiani, H. Müller, and M. Atzori, "Comparison of six electromyography acquisition setups on hand movement classification tasks," *PLoS ONE*, vol. 12, no. 10, Oct. 2017, Art. no. e0186132.

[17] R. N. Khushaba and K. Nazarpour, "Decoding HD-EMG signals for myoelectric control—How small can the analysis window size be?" *IEEE Robot. Autom. Lett.*, vol. 6, no. 4, pp. 8569–8574, Oct. 2021.

[18] S. Planton, M. Jucla, F.-E. Roux, and J.-F. Démonet, "The 'handwriting brain': A meta-analysis of neuroimaging studies of motor versus orthographic processes," *Cortex*, vol. 49, no. 10, pp. 2772–2787, 2013.

[19] L. Pei, M. Longcamp, F. K.-S. Leung, and G. Ouyang, "Temporally resolved neural dynamics underlying handwriting," *NeuroImage*, vol. 244, Dec. 2021, Art. no. 118578.

[20] G. Huang, D. Zhang, X. Zheng, and X. Zhu, "An EMG-based handwriting recognition through dynamic time warping," in *Proc. Annu. Int. Conf. IEEE Eng. Med. Biol.*, Aug. 2010, pp. 4902–4905.

[21] M. Linderman, M. A. Lebedev, and J. S. Erlichman, "Recognition of handwriting from electromyography," *PLoS ONE*, vol. 4, no. 8, p. e6791, Aug. 2009.

[22] J. G. Beltran-Hernandez, J. Ruiz-Pinales, P. Lopez-Rodriguez, J. L. Lopez-Ramirez, and J. G. Avina-Cervantes, "Multi-stroke handwriting character recognition based on sEMG using convolutional-recurrent neural networks," *Math. Biosci. Eng.*, vol. 17, no. 5, pp. 5432–5448, 2020.

[23] A. Phinyomark, P. Phukpattaranont, and C. Limsakul, "Feature reduction and selection for EMG signal classification," *Expert Syst. Appl.*, vol. 39, no. 8, pp. 7420–7431, Jun. 2012.

[24] A. Phinyomark, F. Quaine, S. Charbonnier, C. Serviere, F. Tarpin-Bernard, and Y. Laurillau, "EMG feature evaluation for improving myoelectric pattern recognition robustness," *Expert Syst. Appl.*, vol. 40, no. 12, pp. 4832–4840, Sep. 2013.

[25] A. Tigrini, A. Mengarelli, S. Cardarelli, S. Fioretti, and F. Verdini, "Improving EMG signal change point detection for low SNR by using extended Teager–Kaiser energy operator," *IEEE Trans. Med. Robot. Bionics*, vol. 2, no. 4, pp. 661–669, Nov. 2020.

[26] L. H. Smith, L. J. Hargrove, B. A. Lock, and T. A. Kuiken, "Determining the optimal window length for pattern recognition-based myoelectric control: Balancing the competing effects of classification error and controller delay," *IEEE Trans. Neural Syst. Rehabil. Eng.*, vol. 19, no. 2, pp. 186–192, Apr. 2011.

[27] T. R. Farrell and R. F. Weir, "The optimal controller delay for myoelectric prostheses," *IEEE Trans. Neural Syst. Rehabil. Eng.*, vol. 15, no. 1, pp. 111–118, Mar. 2007.

[28] F. S. Botros, A. Phinyomark, and E. J. Scheme, "Day-to-day stability of wrist EMG for wearable-based hand gesture recognition," *IEEE Access*, vol. 10, pp. 125942–125954, 2022.

[29] M. Asghari Oskoei and H. Hu, "Myoelectric control systems—A survey," *Biomed. Signal Process. Control*, vol. 2, no. 4, pp. 275–294, Oct. 2007.

[30] A. W. Franzke, M. B. Kristoffersen, V. Jayaram, C. K. van der Sluis, A. Murgia, and R. M. Bongers, "Exploring the relationship between EMG feature space characteristics and control performance in machine learning myoelectric control," *IEEE Trans. Neural Syst. Rehabil. Eng.*, vol. 29, pp. 21–30, 2021.

[31] N. E. Bunderson and T. A. Kuiken, "Quantification of feature space changes with experience during electromyogram pattern recognition control," *IEEE Trans. Neural Syst. Rehabil. Eng.*, vol. 20, no. 3, pp. 239–246, May 2012.

[32] N. Nilsson and M. Ortiz-Catalan, "Estimates of classification complexity for myoelectric pattern recognition," in *Proc. 23rd Int. Conf. Pattern Recognit. (ICPR)*, Dec. 2016, pp. 2682–2687.

[33] B. Cesqui, P. Tropea, S. Micera, and H. I. Krebs, "EMG-based pattern recognition approach in post stroke robot-aided rehabilitation: A feasibility study," *J. Neuroeng. Rehabil.*, vol. 10, no. 1, pp. 1–15, 2013.

[34] M. Zardoshti-Kermani, B. C. Wheeler, K. Badie, and R. M. Hashemi, "EMG feature evaluation for movement control of upper extremity prostheses," *IEEE Trans. Rehabil. Eng.*, vol. 3, no. 4, pp. 324–333, Dec. 1995.

[35] I. S. Dhindsa, R. Agarwal, and H. S. Ryait, "Performance evaluation of various classifiers for predicting knee angle from electromyography signals," *Expert Syst.*, vol. 36, no. 3, Jun. 2019, Art. no. e12381.

[36] D. C. Toledo-Pérez, J. Rodríguez-Reséndiz, R. A. Gómez-Loenzo, and J. C. Jauregui-Correa, "Support vector machine-based EMG signal classification techniques: A review," *Appl. Sci.*, vol. 9, no. 20, p. 4402, Oct. 2019.

[37] M. Grandini, E. Bagli, and G. Visani, "Metrics for multi-class classification: An overview," 2020, *arXiv:2008.05756*.

[38] W. Wei, Q. Dai, Y. Wong, Y. Hu, M. Kankanhalli, and W. Geng, "Surface-electromyography-based gesture recognition by multi-view deep learning," *IEEE Trans. Biomed. Eng.*, vol. 66, no. 10, pp. 2964–2973, Oct. 2019.

[39] Y. Z. Arslan, M. A. Adli, A. Akan, and M. B. Baslo, "Prediction of externally applied forces to human hands using frequency content of surface EMG signals," *Comput. Methods Programs Biomed.*, vol. 98, no. 1, pp. 36–44, Apr. 2010.

[40] M. A. Oskoei and H. Hu, "Support vector machine-based classification scheme for myoelectric control applied to upper limb," *IEEE Trans. Biomed. Eng.*, vol. 55, no. 8, pp. 1956–1965, Aug. 2008.

[41] A. L. Hof, "Errors in frequency parameters of EMG power spectra," *IEEE Trans. Biomed. Eng.*, vol. 38, no. 11, pp. 1077–1088, Nov. 1991.
[42] F. Duan, L. Dai, W. Chang, Z. Chen, C. Zhu, and W. Li, "SEMG-based identification of hand motion commands using wavelet neural network combined with discrete wavelet transform," *IEEE Trans. Ind. Electron.*, vol. 63, no. 3, pp. 1923–1934, Mar. 2016.

ANDREA TIGRINI (Member, IEEE) received the M.S. degree in biomedical engineering from Universitã Politecnica delle Marche, Ancona, Italy, in 2018, and the Ph.D. degree in information engineering, in 2022. He is currently a Postdoctoral Research Fellow with the Department of Information Engineering, Università Politecnica delle Marche. His research interests include human biomechanics, neuromuscular control, myoelectric pattern recognition, and rehabilitation engineering. In these fields, he has authored/coauthored scientific publications in international journals and conference proceedings.

FEDERICA VERDINI (Member, IEEE) received the M.S. degree in electronic engineering from Ancona University, Ancona, Italy, in 1997, and the Ph.D. degree in bioengineering from Bologna University, Bologna, Italy, in 2001. She is currently the Chief-Staff Scientist of the Movement Analysis and Bioengineering Laboratory, Università Politecnica delle Marche, Ancona. Her research interests include recording and processing of biological signals associated with human movement and the study of control models related to motion and posture. In these fields, she has authored many scientific publications in international journals, books, and conference proceedings.

MARA SCATTOLINI (Graduate Student Member, IEEE) received the M.Sc. degree (cum laude) in biomedical engineering from Università Politecnica delle Marche, Ancona, Italy, in 2022, where she is currently pursuing the Ph.D. degree in information engineering with the Department of Information Engineering. Her thesis focused on the development of a framework for multi-user gesture recognition from EMG data.

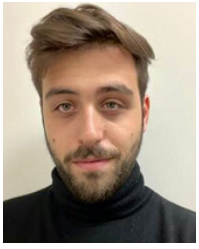

FEDERICO BARBAROSSA received the M.Sc. degree (cum laude) in biomedical engineering from Università Politecnica delle Marche, Ancona, Italy, in 2021. His thesis focused on data acquisition and processing for handwriting recognition. From 2021 to 2022, he was with the Department of Information Engineering of Università Politecnica delle Marche. He is currently a Research Associate with IRCCS, Ancona. His current research interest includes application of artificial intelligence in medical prognosis and diagnosis.

LAURA BURATTINI (Member, IEEE) cofounded and managed the academic spin-off B.M.E.D. Bio-Medical Engineering Development Srl, as the CEO and the President, from 2012 to 2016. She is currently a Full Professor of bioengineering and the President of the Biomedical Engineering Degree Council, Università Politecnica delle Marche, Italy, where she manages the Cardiovascular Bioengineering Laboratory and the Bioengineering Laboratory. Her research interests include processing and modeling of biomedical signals, especially of the cardiovascular, metabolic and motor systems.

MICAELA MORETTINI (Member, IEEE) received the M.S. degree in biomedical engineering from the University of Bologna, in 2008, and the Ph.D. degree in electromagnetics and bioengineering from Università Politecnica delle Marche (UNIVPM), in 2012. She was also the Co-Founder of the academic spin-off company B.M.E.D. Bio-Medical Engineering Development Srl, UNIVPM, for which she was the Vice-President and then as the President. She is currently an Assistant Professor of bioengineering with the Department of Information Engineering, UNIVPM, where she teaches "models and control of biological systems" for the master's degree course (held in English language) of "biomedical engineering." Her main expertise is on developing mathematical models and methods for quantitative physiology for the description of glucose-insulin regulatory systems and its alterations leading to Type 2 Diabetes. She also works on describing, through mathematical modeling, the effects of physical exercise on the endocrine-metabolic system. She was involved in several national research projects and in the EU-FP7 project MISSION T2D. Her research interests include the field of the biomedical informatics and, in particular, the development of approaches for clinical decision support using electronic health records data aimed to Type 2 Diabetes diagnosis, management and prevention. She is a member of the IEEE-EMBS, National Bioengineering Group, and the Italian Society of Diabetology.

SANDRO FIORETTI (Member, IEEE) received the M.S. degree in electronic engineering from Ancona University, Ancona, Italy, in 1979. He is currently an Associate Professor of bioengineering with the Department of Information Engineering, Università Politecnica delle Marche, Ancona, where he teaches movement biomechanics and bioengineering of motor rehabilitation at the biomedical engineering course. He has participated in various European and national research projects in the field of movement analysis for motor rehabilitation. He is the author of numerous scientific publications in international journals, books, and congress proceedings. His main research interests include the field of human movement analysis and its related fields, such as stereophotogrammetry, linear and nonlinear filtering, joint kinematics, analysis and identification of postural control, static and perturbed posturography, gait analysis, and dynamic electromyography.

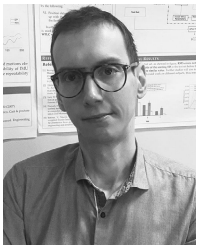

ALESSANDRO MENGARELLI (Member, IEEE) received the M.S. degree in biomedical engineering and the Ph.D. degree in information engineering from Università Politecnica delle Marche, Ancona, Italy, in 2012 and 2017, respectively. He is currently an Assistant Professor with the Department of Information Engineering, Universitã Politecnica delle Marche. His current research interests include biomechanics of movement in both static and dynamic conditions, application of control theory and modeling to the analysis of balance, and nonlinear analysis of time series. Furthermore, he is also involved in the assessment of muscular functions during gait and in myoelectric pattern recognition for upper and lower limb prosthetic control. In these fields, he authored/coauthored scientific publications in peer-reviewed international journals and conference proceedings.

Open Access funding provided by 'Università Politecnica delle Marche' within the CRUI CARE Agreement